Tunable SIM properties in a family of 3D anilato-based Lanthanide-MOFs

Noemi Monni,[a,b] Sourav Dey,[a] Víctor García-López,[a] Mariangela Oggianu,[b] José J. Baldoví,[a] Maria Laura Mercuri,[b] Miguel Clemente-León,[a*] and Eugenio Coronado[a]*

[a] Instituto de Ciencia Molecular (ICMol), Universidad de Valencia, Catedrático José Beltrán 2, 46980 Paterna, Spain

[b] Dipartimento di Scienze Chimiche e Geologiche, Università degli Studi di Cagliari, Complesso Universitario di Monserrato, 09042 Monserrato, Italy

Table of Contents

1. Elemental Analysis

1.1 Table S1. Elemental analysis for all the compounds **1-3a** and **1-3b**.

		Calculated			Found		
		%C	**%H**	**%N**	**%C**	**%H**	**%N**
1a	$C_{30}H_{40}N_{18}O_{26}Dy_2$	25.85	2.89	18.09	25.39	2.80	18.12
1b	$C_{30}H_{34}N_{18}O_{23}Dy_2$	26.90	2.56	18.81	26.54	2.36	17.47
2a	$C_{30}H_{40}N_{18}O_{26}Tb_2$	25.99	2.91	18.18	25.85	2.75	18.23
2b	$C_{30}H_{34}N_{18}O_{23}Tb_2$	27.04	2.57	18.92	25.52	2.27	19.41
3a	$C_{30}H_{40}N_{18}O_{26}Ho_2$	25.76	2.88	18.03	25.79	2.67	18.10
3b	$C_{30}H_{34}N_{18}O_{23}Ho_2$	26.80	2.55	18.75	26.93	2.33	19.11

1. Crystal Structure

1.1 **Table S2**. Crystallographic data for compounds **1-3a.**

	1a	**2a**	**3a**
Empirical formula	$C_{30}H_{38}N_{18}O_{25}Dy_2$	$C_{30}H_{38}N_{18}O_{25}Tb_2$	$C_{30}H_{38}N_{18}O_{25}Ho_2$
FW	1365.65	1358.50	1370.51
Crystal color	Dark Red	Dark Red	Dark Red
Crystal size (mm^3)	0.22 × 0.16 × 0.13	0.17 × 0.14 × 0.11	0.2 × 0.16 × 0.08
Temperature (K)	120	120	120
Wavelength (Å)	(MoKa) λ = 0.71073	(MoKa) λ = 0.71073	(MoKa) λ = 0.71073
Crystal system	triclinic	triclinic	Triclinic
Space group	*P-1*	*P-1*	*P-1*
a (Å)	8.9737 (4)	8.9903(4)	8.9571 (3)
b (Å)	9.4011 (4)	9.4164(4)	9.4084 (3)
c (Å)	15.5290 (6)	15.5861(6)	15.4980 (4)
α (°)	75.273 (4)	75.214(3)	75.173 (2)
β (°)	77.475 (4)	77.435(4)	77.349 (2)
γ (°)	68.042 (4)	68.017(4)	67.977 (3)
V (Å³)	1164.23 (9)	1172.01(9)	1159.35 (7)
ρ_{calc} ($g.cm^{-3}$)	1.962	1.939	1.977
μ(MoKα) (mm^{-1})	3.293	3.100	3.496
2θ range (°)	6.516 to 56.212	6.514 to 55.868	6.626 to 54.962
Index ranges	-11 ≤ h ≤ 11, -12 ≤ k ≤ 11, -20 ≤ l ≤ 19	-11 ≤ h ≤ 11, -12 ≤ k ≤ 11, -18 ≤ l ≤ 20	-10 ≤ h ≤ 11, -11 ≤ k ≤ 12, -20 ≤ l ≤ 19
Reflections collected	17487	15479	16014
Independent reflections	4931 [R_{int} = 0.0259, R_{sigma} = 0.0264]	4908 [R_{int} = 0.0406, R_{sigma} = 0.0517]	4772 [R_{int} = 0.0238, R_{sigma} = 0.0218]
Data/restraints/parameters	4931/0/359	4908/0/384	4772/0/359
Goodness-of-fit on F2	1.070	1.054	1.033
Final R indexes [I>=2σ (I)]	R_1 = 0.0199 wR_2 = 0.0451	R_1 = 0.0290, wR_2 = 0.0562	R_1 = 0.0184 wR_2 = 0.0457
Final R indexes [all data]	R_1 = 0.0213 wR_2 = 0.0459	R_1 = 0.0355, wR_2 = 0.0602	R_1 = 0.0189 wR_2 = 0.0461
Largest diff.peak/hole/e $Å^{-3}$	0.90/-0.83	1.01/-0.80	0.80/-0.80

1.2 **Table S3**. Crystallographic data for compounds 1-**3b.**

	1b	**2b**	**3b**
Empirical formula	$C_{30}H_{28}N_{18}O_{20}Dy_2$	$C_{30}H_{28}N_{18}O_{20}Tb_2$	$C_{30}H_{28}N_{18}O_{20}Ho_2$
FW	1285.65	1278.50	1290.51
Crystal color	Orange	Orange	Orange
Crystal size (mm^3)	0.14 × 0.09 × 0.08	0.16 × 0.14 × 0.07	0.29 × 0.13 × 0.09
Temperature (K)	120	120	120
Wavelength (Å)	(MoKa) λ = 0.71073	(MoKa) λ = 0.71073	(MoKa) λ = 0.71073
Crystal system	triclinic	triclinic	triclinic
Space group	*P-1*	*P-1*	*P-1*
a (Å)	8.6480 (4)	8.6577(2)	8.6344 (2)
b (Å)	10.4211 (5)	10.4166(3)	10.4202 (2)
c (Å)	12.0603 (6)	12.0856(4)	12.0281 (3)
α (°)	80.197 (4)	80.206(2)	80.171 (2)
β (°)	79.454 (4)	79.607(2)	79.315 (2)
γ (°)	82.476 (4)	82.473(2)	82.353 (2)
V (Å³)	1047.33 (9)	1050.75(5)	1042.06 (4)
ρ_{calc} ($g.cm^{-3}$)	2.038	2.021	2.057
μ(MoKα) (mm^{-1})	3.644	3.442	3.874
2θ range (°)	6.564 to 60.882	6.56 to 61.078	6.974 to 60.86
Index ranges	$-12 \le h \le 12$, $-14 \le k \le 14$, $-16 \le l \le 16$	$-11 \le h \le 12$, $-13 \le k \le 14$, $-16 \le l \le 16$	$-12 \le h \le 12$, $-14 \le k \le 14$, $-16 \le l \le 16$
Reflections collected	17270	20971	20633
Independent reflections	5565 [R_{int} = 0.0503, R_{sigma} = 0.0609]	5718 [R_{int} = 0.0316, R_{sigma} = 0.0325]	5678 [R_{int} = 0.0255, R_{sigma} = 0.0247]
Data/restraints/parameters	5565/0/324	5718/0/324	5678/0/324
Goodness-of-fit on F2	1.052	1.065	1.060
Final R indexes [I>=2σ (I)]	R_1 = 0.0312, wR_2 = 0.0550	R_1 = 0.0201, wR_2 = 0.0441	R_1 = 0.0166, wR_2 = 0.0366
Final R indexes [all data]	R_1 = 0.0385, wR_2 = 0.0592	R_1 = 0.0221, wR_2 = 0.0454	R_1 = 0.0175, wR_2 = 0.0370
Largest diff. peak/hole/$eÅ^{-3}$	0.86/-0.95	0.92/-0.74	0.74/-0.69

$[Ln_2(trz_2An)_3(H_2O)_4]_n \cdot 10H_2O$ (Ln^{III} = Dy, Tb, Ho), Phase A

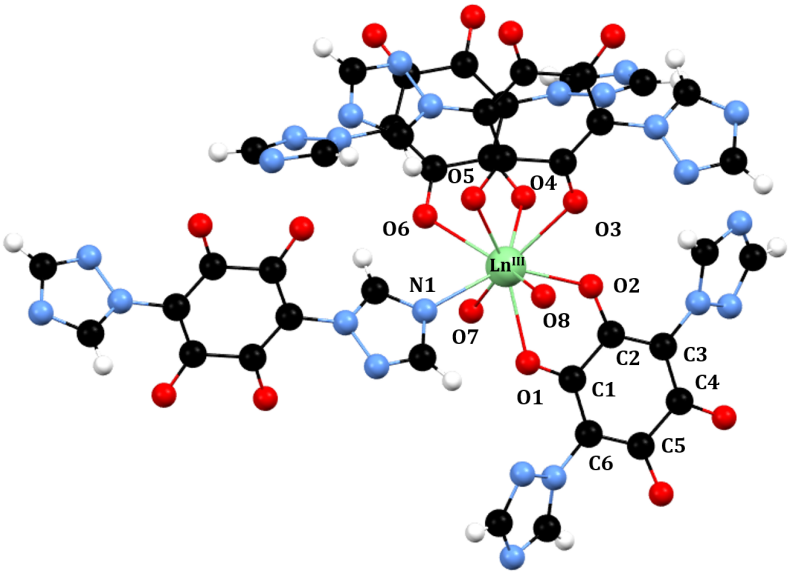

1.3 **Table S4** Selected bond lengths and angles for $[Dy_2(trz_2An)_3(H_2O)_4]_n$ $10H_2O$ **(1a)**

Bonds	Å	Angles	°	Angles	°
Dy– O1	2.4253(16)	**N1 – Dy – O1**	75.82(6)	**O2 – Dy – O6**	134.38(6)
Dy – O2	2.3449(16)	**N1 – Dy – O2**	141.57(6)	**O2 – Dy – O7**	84.32(6)
Dy – O3	2.4303(17)	**N1 – Dy – O3**	134.56(6)	**O2 – Dy – O8**	87.99(6)
Dy – O4	2.4007(18)	**N1 – Dy – O4**	137.20(7)	**O3 – Dy – O4**	68.95(6)
Dy – O5	2.4511(17)	**N1 – Dy – O5**	76.46(6)	**O3 – Dy – O5**	64.82(6)
Dy – O6	2.4516(17)	**N1 – Dy – O6**	72.86(6)	**O3 – Dy – O6**	108.60(6)
Dy – O7	2.3924(19)	**N1 – Dy – O7**	80.64(7)	**O3 – Dy – O7**	144.32(6)
Dy – O8	2.3976(18)	**N1 – Dy – O8**	78.72(7)	**O3 – Dy – O8**	69.86(6)
Dy – N1	2.491(2)	**O1 – Dy – O2**	65.77(6)	**O4 – Dy – O5**	91.41(6)
C1 – O1	1.253(3)	**O1 – Dy – O3**	118.56(6)	**O4 – Dy – O6**	64.88(6)
C2 – O2	1.256(3)	**O1 – Dy – O4**	130.16(6)	**O4 – Dy – O7**	80.24(6)
C1 – C2	1.534(3)	**O1 – Dy – O5**	137.86(6)	**O4 – Dy – O8**	138.45(6)
C2 – C3	1.394(3)	**O1 – Dy – O6**	132.79(6)	**O5 – Dy – O6**	65.21(6)
		O1 – Dy – O7	68.92(6)	**O5 – Dy – O7**	135.53(6)
		O1 – Dy – O8	67.97(6)	**O5 – Dy – O8**	75.94(6)
		O2 – Dy – O3	70.20(6)	**O6 – Dy – O7**	71.83(6)
		O2 – Dy – O4	73.27(6)	**O6 – Dy – O8**	135.93(6)
		O2 – Dy – O5	135.01(6)	**O7 – Dy – O8**	135.48(6)

1.4 **Table S5** Selected bond lengths and angles for $[Tb_2(trz_2An)_3(H_2O)_4]_n$ $10H_2O$ **(2a)**

Bonds	Å	Angles	°	Angles	°
Tb– O1	2.439(2)	**N1 – Tb – O1**	76.03(8)	**O2 – Tb – O6**	134.42(8)
Tb – O2	2.353(2)	**N1 – Tb – O2**	141.50(8)	**O2 – Tb – O7**	84.47(9)
Tb – O3	2.413(2)	**N1 – Tb – O3**	137.00(9)	**O2 – Tb – O8**	87.96(8)
Tb – O4	2.438(2)	**N1 – Tb – O4**	134.35(9)	**O3 – Tb – O4**	69.02(8)
Tb – O5	2.468(2)	**N1 – Tb – O5**	76.51(8)	**O3 – Tb – O5**	91.21(8)
Tb – O6	2.459(2)	**N1 – Tb – O6**	72.97(9)	**O3 – Tb – O6**	64.53(8)
Tb – O7	2.406(3)	**N1 – Tb – O7**	80.31(9)	**O3 – Tb – O7**	72.08(9)
Tb – O8	2.415(2)	**N1 – Tb – O8**	78.46(9)	**O3 – Tb – O8**	138.75(8)
Tb – N1	2.504(3)	**O1 – Tb – O2**	65.49(7)	**O4 – Tb – O5**	64.48(8)
C1 – O1	1.251(4)	**O1 – Tb – O3**	130.27(8)	**O4 – Tb – O6**	108.47(8)
C2 – O2	1.253(4)	**O1 – Tb – O4**	118.54(8)	**O4 – Tb – O7**	144.88(8)
C1 – C2	1.545(4)	**O1 – Tb – O5**	137.91(8)	**O4 – Tb – O8**	70.07(8)
C2 – C3	1.393(4)	**O1 – Tb – O6**	132.93(8)	**O5 – Tb – O6**	65.47(9)
C3 – C4	1.392(5)	**O1 – Tb – O7**	68.45(8)	**O5 – Tb – O7**	135.89(8)
		O1 – Tb – O8	67.85(8)	**O5 – Tb – O8**	75.85(8)
		O2 – Tb – O3	73.69(8)	**O6 – Tb – O7**	80.86(8)
		O2 – Tb – O4	70.36(8)	**O6 – Tb – O8**	135.98(8)
		O2 – Tb – O5	134.82(8)	**O7 – Tb – O8**	134.76(8)

1.5 **Table S6.** Selected bond lengths and angles for $[Ho_2(trz_2An)_3(H_2O)_4]_n$ $10H_2O$ **(3a)**

Bonds	Å	Angles	°	Angles	°
Ho – O1	2.4205(16)	**N1 – Ho – O1**	75.50(6)	**O2 – Ho – O6**	134.38(6)
Ho – O2	2.4440(17)	**N1 – Ho – O2**	141.45(6)	**O2 – Ho – O7**	83.76(6)
Ho – O3	2.3303(16)	**N1 – Ho – O3**	134.80(6)	**O2 – Ho – O8**	88.07(6)
Ho – O4	2.4211(16)	**N1 – Ho – O4**	137.23(6)	**O3 – Ho – O4**	68.85(6)
Ho – O5	2.3882(7)	**N1 – Ho – O5**	76.48(6)	**O3 – Ho – O5**	64.99(5)
Ho – O6	2.4434(17)	**N1 – Ho – O6**	72.79(6)	**O3 – Ho – O6**	108.76(6)
Ho – O7	2.3887(17)	**N1 – Ho – O7**	80.92(6)	**O3 – Ho – O7**	143.85(6)
Ho – O8	2.3838(18)	**N1 – Ho – O8**	78.81(6)	**O3 – Ho – O8**	69.82(6)
Ho – N1	2.471(2)	**O1 – Ho – O2**	65.98(5)	**O4 – Ho – O5**	91.54(6)
C1 – O1	1.247(3)	**O1 – Ho – O3**	118.68(5)	**O4 – Ho – O6**	64.99(6)
C2 – O2	1.253(3)	**O1 – Ho – O4**	130.34(6)	**O4 – Ho – O7**	80.12(6)
C1 – C2	1.539(3)	**O1 – Ho – O5**	137.59(6)	**O4 – Ho – O8**	138.33(6)
C2 – C3	1.395(3)	**O1 – Ho – O6**	132.51(6)	**O5 – Ho – O6**	65.34(6)
		O1 – Ho – O7	68.70(6)	**O5 – Ho – O7**	136.00(6)
		O1 – Ho – O8	68.07(6)	**O5 – Ho – O8**	75.74(6)
		O2 – Ho – O3	70.15(6)	**O6 – Ho – O7**	135.88(6)
		O2 – Ho – O4	73.24(6)	**O6 – Ho – O8**	72.12(6)
		O2 – Ho – O5	135.11(6)	**O7 – Ho – O8**	135.53(6)

$Ln_2(trz_2An)_3(H_2O)_4]_n \cdot 7H_2O$ (Ln^{III} = Dy, Tb, Ho), Phase B

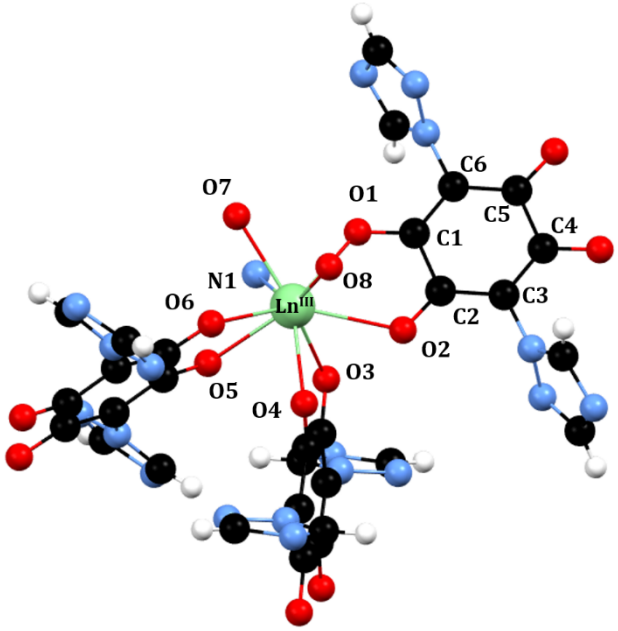

1.6 **Table S7**. Selected bond lengths and angles for $[Dy_2(trz_2An)_3(H_2O)_4]_n$ $7H_2O$ **(1b)**

Bonds	Å	Angles	°	Angles	°
Dy– O1	2.358(2)	**N1 – Dy – O1**	70.81(8)	**O2 – Dy – O6**	127.08(7)
Dy – O2	2.503(2)	**N1 – Dy – O2**	116.94(8)	**O2 – Dy – O7**	131.99(8)
Dy – O3	2.417(2)	**N1 – Dy – O3**	70.98(8)	**O2 – Dy – O8**	70.28(8)
Dy – O4	2.378(2)	**N1 – Dy – O4**	129.79(8)	**O3 – Dy – O4**	67.26(7)
Dy – O5	2.417(2)	**N1 – Dy – O5**	67.10(8)	**O3 – Dy – O5**	70.84(8)
Dy – O6	2.517(2)	**N1 – Dy – O6**	115.39(8)	**O3 – Dy – O6**	124.65(7)
Dy – O7	2.369(2)	**N1 – Dy – O7**	142.35(9)	**O3 – Dy – O7**	136.44(8)
Dy – O8	2.359(2)	**N1 – Dy – O8**	72.99(8)	**O3 – Dy – O8**	143.96(8)
Dy – N1	2.551(3)	**O1 – Dy – O2**	65.16(7)	**O4 – Dy – O5**	73.74(8)
C1 – O1	1.252(4)	**O1 – Dy – O3**	92.00(8)	**O4 – Dy – O6**	70.54(8)
C2 – O2	1.246(4)	**O1 – Dy – O4**	135.71(8)	**O4 – Dy – O7**	87.85(8)
C1 – C2	1.531(4)	**O1 – Dy – O5**	137.71(8)	**O4 – Dy – O8**	141.65(8)
C2 – C3	1.408(4)	**O1 – Dy – O6**	143.25(8)	**O5 – Dy – O6**	64.10(7)
		O1 – Dy – O7	81.40(8)	**O5 – Dy – O7**	94.58(8)
		O1 – Dy – O8	76.74(8)	**O5 – Dy – O8**	137.36(8)
		O2 – Dy – O3	67.97(8)	**O6 – Dy – O7**	71.52(8)
		O2 – Dy – O4	70.74(7)	**O6 – Dy – O8**	73.61(8)
		O2 – Dy – O5	133.26(8)	**O7 – Dy – O8**	76.33(8)

1.7 **Table S8**. Selected bond lengths and angles for $[Tb_2(trz_2An)_3(H_2O)_4]_n$ $7H_2O$ **(2b)**

Bonds	Å	Angles	°	Angles	°
Tb– O1	2.4014(14)	**N1 – Tb – O1**	67.11(5)	**O2 – Tb – O6**	143.30(5)
Tb – O2	2.5260(15)	**N1 – Tb – O2**	115.20(5)	**O2 – Tb – O7**	71.85(5)
Tb – O3	2.4279(15)	**N1 – Tb – O3**	70.98(6)	**O2 – Tb – O8**	74.63(5)
Tb – O4	2.3900(15)	**N1 – Tb – O4**	129.57(5)	**O3 – Tb – O4**	66.92(5)
Tb – O5	2.5086(15)	**N1 – Tb – O5**	116.84(5)	**O3 – Tb – O5**	68.19(5)
Tb – O6	2.3707(15)	**N1 – Tb – O6**	70.75(5)	**O3 – Tb – O6**	92.42(5)
Tb – O7	2.3817(17)	**N1 – Tb – O7**	72.79(6)	**O3 – Tb – O7**	143.77(5)
Tb – O8	2.3672(15)	**N1 – Tb – O8**	141.80(6)	**O3 – Tb – O8**	136.43(5)
Tb – N1	2.5664(18)	**O1 – Tb – O2**	63.86(5)	**O4 – Tb – O5**	70.91(5)
C1 – O1	1.255(2)	**O1 – Tb – O3**	70.52(5)	**O4 – Tb – O6**	135.91(5)
C2 – O2	1.246(2)	**O1 – Tb – O4**	73.56(5)	**O4 – Tb – O7**	142.03(5)
C1 – C2	1.531(3)	**O1 – Tb – O5**	133.27(5)	**O4 – Tb – O8**	88.62(5)
C2 – C3	1.402(3)	**O1 – Tb – O6**	137.67(5)	**O5 – Tb – O6**	65.20(5)
		O1 – Tb – O7	94.69(6)	**O5 – Tb – O7**	131.83(5)
		O1 – Tb – O8	138.18(5)	**O5 – Tb – O8**	69.92(5)
		O2 – Tb – O3	124.15(5)	**O6 – Tb – O7**	76.34(5)
		O2 – Tb – O4	70.58(5)	**O6 – Tb – O8**	80.57(5)
		O2 – Tb – O5	127.34(5)	**O7 – Tb – O8**	76.36(6)

1.8 **Table S9**. Selected bond lengths and angles for $[Ho_2(trz_2An)_3(H_2O)_4]_n \cdot 7H_2O$ **(3b)**

Bonds	Å	Angles	°	Angles	°
Ho – O1	2.3793(13)	**N1 – Ho – O1**	67.20(5)	**O2 – Ho – O6**	142.96(4)
Ho – O2	2.5081(13)	**N1 – Ho – O2**	115.55(5)	**O2 – Ho – O7**	71.39(5)
Ho – O3	2.4052(13)	**N1 – Ho – O3**	70.99(5)	**O2 – Ho – O8**	74.02(5)
Ho – O4	2.3647(13)	**N1 – Ho – O4**	130.15(5)	**O3 – Ho – O4**	67.57(4)
Ho – O5	2.4956(13)	**N1 – Ho – O5**	117.06(5)	**O3 – Ho – O5**	68.01(4)
Ho – O6	2.3487(13)	**N1 – Ho – O6**	70.49(5)	**O3 – Ho – O6**	91.99(4)
Ho – O7	2.3547(13)	**N1 – Ho – O7**	72.84(5)	**O3 – Ho – O7**	143.82(5)
Ho – O8	2.3405(13)	**N1 – Ho – O8**	141.78(5)	**O3 – Ho – O8**	136.32(5)
Ho – N1	2.5396(16)	**O1 – Ho – O2**	64.27(4)	**O4 – Ho – O5**	70.57(4)
C1 – O1	1.252(2)	**O1 – Ho – O3**	70.97(4)	**O4 – Ho – O6**	135.94(4)
C2 – O2	1.246(2)	**O1 – Ho – O4**	73.96(5)	**O4 – Ho – O7**	141.50(5)
C1 – C2	1.529(3)	**O1 – Ho – O5**	133.31(4)	**O4 – Ho – O8**	88.05(5)
C2 – C3	1.404(2)	**O1 – Ho – O6**	137.51(5)	**O5 – Ho – O6**	65.56(4)
		O1 – Ho – O7	94.38(5)	**O5 – Ho – O7**	132.15(5)
		O1 – Ho – O8	137.98(5)	**O5 – Ho – O8**	69.87(5)
		O2 – Ho – O3	124.94(4)	**O6 – Ho – O7**	76.59(5)
		O2 – Ho – O4	70.51(4)	**O6 – Ho – O8**	80.86(5)
		O2 – Ho – O5	126.83(4)	**O7 – Ho – O8**	76.37(5)

1-3a and **1-3b** polycrystalline samples are pure and homogeneous, proving to be perfectly consistent with the calculated pattern from CIF and isostructural to the corresponding Er^{III}-based frameworks[1] (**Figure S1**).

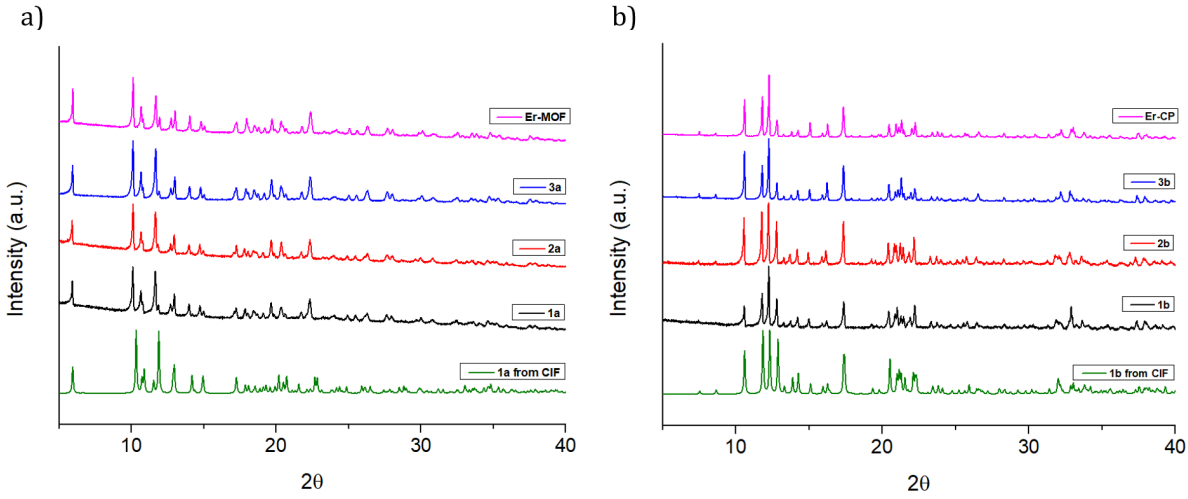

1.9 **Figure S1**. Experimental and calculated PXRD patterns in 2θ range of 5-40° for **1-3a** (a) and for **1-3b** (b), compared with the respective Er^{III}-coordination networks of phase a and b (magenta lines).

2. FT-IR Spectroscopy

FT-IR spectra of **1-3a** and **1-3b** were performed and compared with H_2trz_2An linker to further confirm the coordination between trz_2An and Ln^{III} ion. **1-3a** and **1-3b** spectra are here reported, with the principal band assignment for 1a and 1b as representative of the corresponding series (**Table S10**). As shown in **Figure S2**, the band at 1650 cm^{-1} of nC-O of free ligand disappear and the broad band centered at 1550 cm^{-1} is downshifted, due to the coordination of C-O in the frameworks. Below 460 cm^{-1} the typical bands related to the nLn-O stretching vibrations are present, due to the coordination bonds.

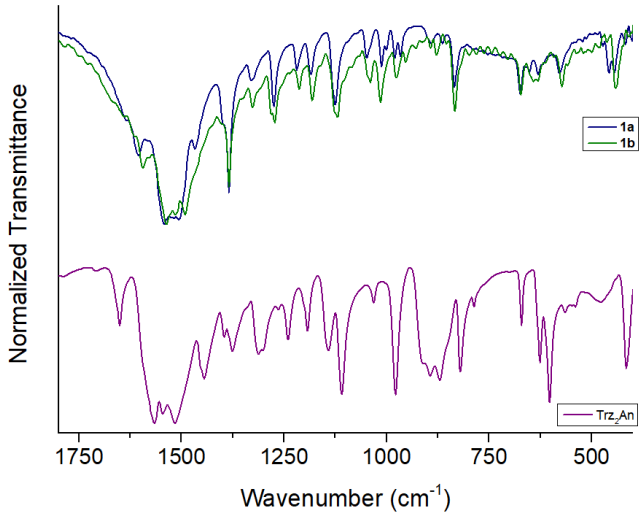

2.1 **Figure S2.** FT-IR spectra of **H2trz2An** (purple), **1a** (blue) **a**nd **1b** (green) in the 1800-400 cm^{-1} region.

2.2 **Table S10.** Assignments of characteristic bands for **1a** and **1b**, all the frequencies are in cm^{-1}.[3–6]

	1a	**1b**
ν O-H	3388	3438
ν C=O	1605	1589
ν C=O + ν C=C aromatic	1513 1492	1506 1488
ν aromatic ring	1385	1391 1377
ν C-N	1321 1272	1325 1278 1272
ν N-N	1183	1181
δ C=C	835	835
ν Dy-O	459 446	438

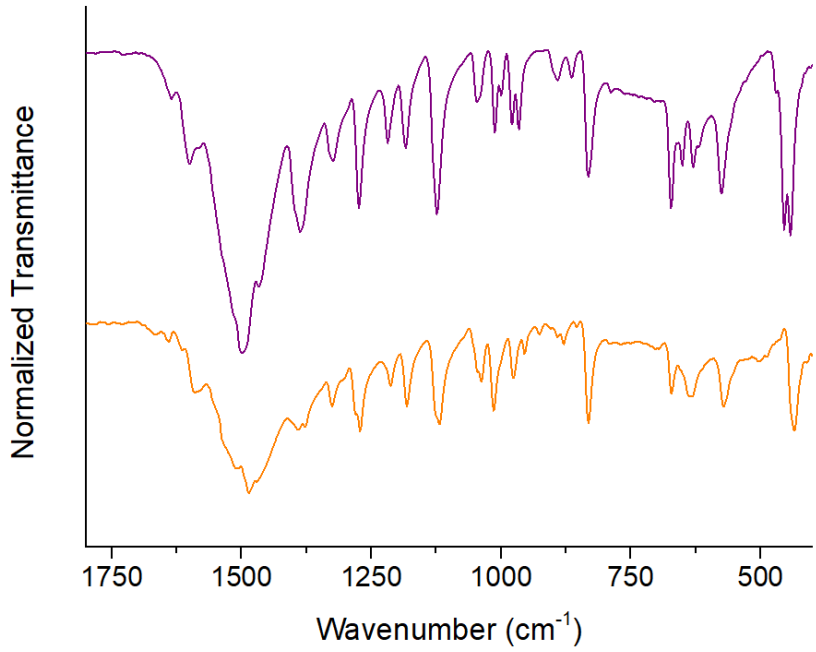

2.3 **Figure S3.** FT-IR spectra of **2a** (purple line) and **2b** (orange line) in 1800-400 cm^{-1} range.

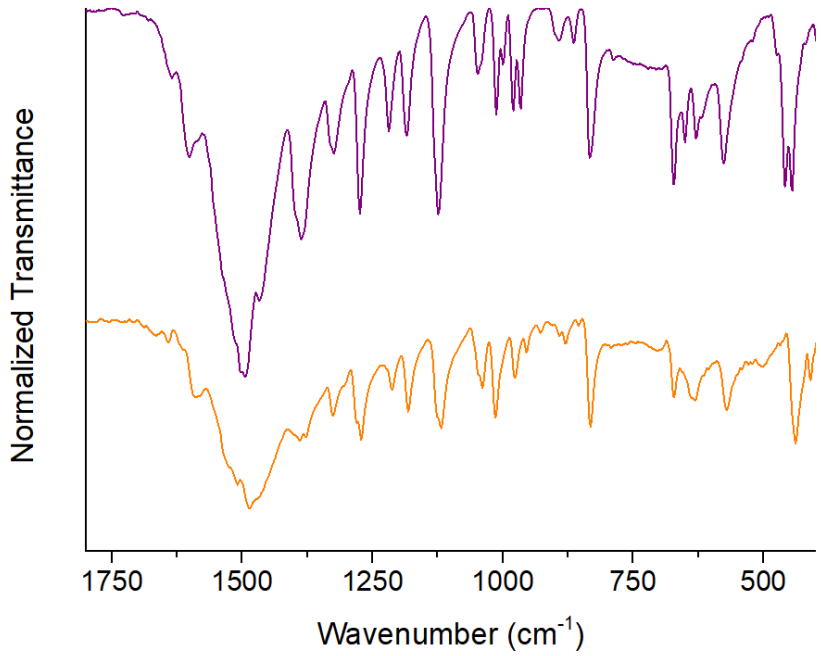

2.4 **Figure S4**. FT-IR spectra of **3a** (purple line) and **3b** (orange line) in 1800-400 cm^{-1} range.

3. Magnetic Properties and Theoretical Calculations

3.1 **Table S11**. The CASSCF/RASSI-SO/SINGLE_ANISO computed energy and g tensors of the $^6H_{15/2}$ KDs **for 1a**.

Energy (cm^{-1})	g_{xx}	g_{yy}	g_{zz}
0.0	0.140	0.244	18.777
71.6	2.889	6.253	11.751
102.5	7.901	5.375	0.398
154.9	1.866	3.560	10.498
192.9	0.821	3.614	14.433
222.3	1.622	3.232	11.996
263.1	0.773	1.110	16.893
312.7	0.262	0.340	19.031

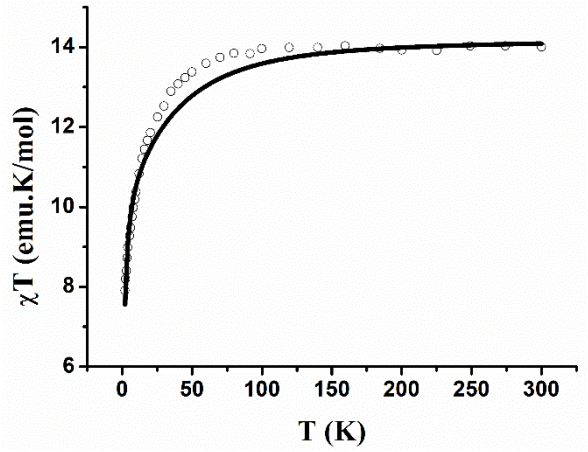

3.2 **Figure S5.** A comparison of experimental and computed temperature dependent magnetization of **1a**. A dipolar coupling (zJ) of -0.12 cm^{-1} was considered in our calculations to simulate the experimental magnetic data. The experimental data has been scaled with a factor of 0.90. We have added TIP (temperature independent paramagnetism) value of 0.003 emu/mol to correct the experimental χT value of **1a**.

3.3 **Table S12.** The CASSCF/RASSI-SO/SINGLE_ANISO computed energy and g tensors of the 6H15/2 KDs for **1a_des**.

Energy (cm^{-1})	g_{xx}	g_{yy}	g_{zz}
0.0	0.002	0.006	19.328
139.1	0.101	0.163	15.950
264.9	9.641	6.526	2.764
307.1	10.941	5.960	0.333
325.6	0.574	2.462	12.357
385.8	1.789	2.223	13.321
426.9	0.316	0.359	15.546
554.4	0.009	0.019	19.456

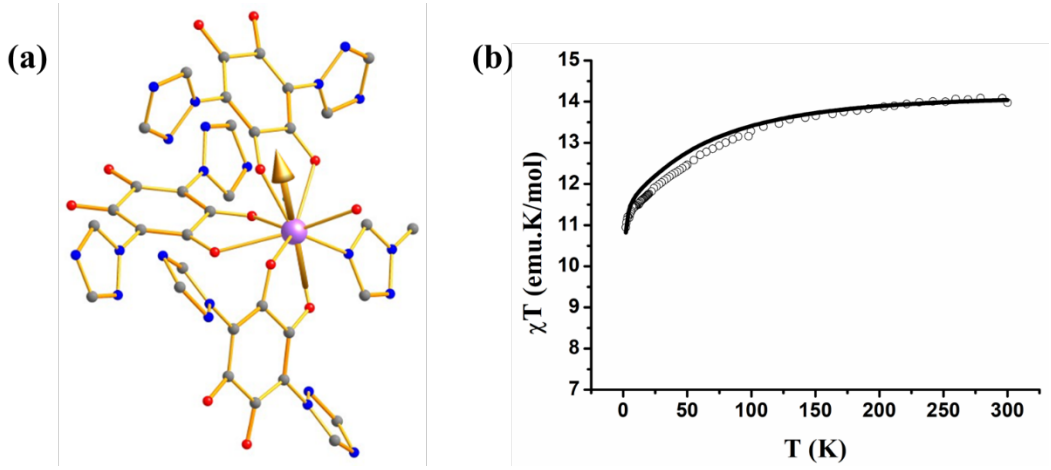

3.4 **Figure S6.** (a) The anisotropy axis of KD1 of **1a_des.** Colour code: Dy:purple, O:red, N:blue, C:grey. Hydrogens are omitted for clarity. (b) A comparison of experimental and computed temperature dependent magnetization of **1a_des**. The experimental data has been scaled with a factor of 0.90. We have added TIP (temperature independent paramagnetism) value of 0.005 emu/mol to correct the experimental χT value of **1a_des**. A dipolar coupling (zJ) of -0.02 cm^{-1} was considered in our calculations to simulate the experimental magnetic data.

3.5 **Table S13.** The CASSCF/RASSI-SO/SINGLE_ANISO computed energy and g tensors of the $^6H_{15/2}$ KDs for **1b**.

Energy (cm^{-1})	g_{xx}	g_{yy}	g_{zz}
0.0	0.021	0.041	19.547
102.6	0.412	0.521	18.352
145.6	3.231	4.950	12.319
184.0	1.326	5.552	10.358
243.3	0.113	1.917	15.031
304.9	10.597	6.814	1.728
348.7	2.364	4.755	10.862
401.0	0.581	2.383	17.762

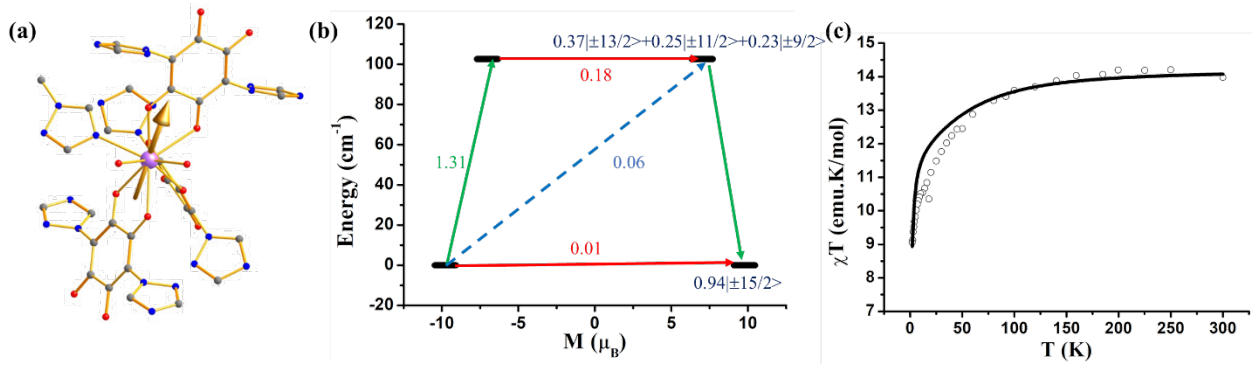

3.6 **Figure S7**. (a) The anisotropy axis of KD1 of 1b. Colour code: Dy:purple, O:red, N:blue, C:grey. Hydrogens are omitted for clarity. (b) The energy vs magnetic moment for J = 15/2 ground state of Dy in **1b**. The red arrow represents QTM via ground state and TA-QTM via first excited state. The sky blue dotted arow represent the Orbach process. The green arrow shows possible mechanism of magnetization relaxation. (c) A comparison of experimental and computed temperature dependent magnetization of **1b**. A dipolar coupling (zJ) of -0.08 cm^{-1} was considered in our calculations to simulate the experimental magnetic data. The computed data has been scaled with a scaling factor of 1.1 for **1b**.

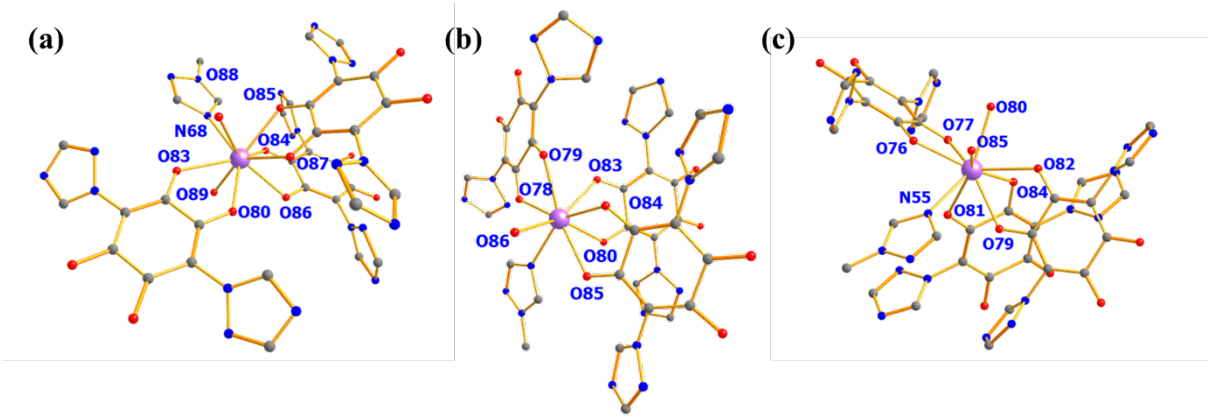

3.7 **Figure S8.** Loprop charge model of (a) **1a**, (b) **1a_des** and (c) **1b** for Table S14. Colour code: Dy:purple, O:red, N:blue, C:grey. Hydrogens are omitted for clarity.

3.8 **Table S14.** The CASSCF computed Loprop charges metal and atoms in the first coordination sphere of **1a, 1a_des** and **1b.**

Atom	**1a**	**Atom**	**1a_des**	**Atom**	**1b**
Dy	2.5196	Dy	2.5178	Dy	2.5176
O80	-0.6985	O78	-0.7488	O76	-0.7443
O83	-0.7128	O79	-0.7182	O77	-0.6576
O84	-0.6728	O80	-0.7339	O79	-0.7263

O85	-0.7278	O83	-0.6796	O80	-0.7085
O86	-0.6991	O84	-0.7536	O81	-0.6925
O87	-0.7211	O85	-0.6925	O82	-0.7204
O88	-0.6959	O86	-0.6898	O84	-0.7179
O89	-0.6761	N67	-0.4347	O85	-0.6910
N68	-0.4321			N55	-0.3976

3.9 **Table S15**. The computed crystal field parameters (B_k^q; Stevens notation) in cm^{-1} obtained for **1a**, **1a_des** and **1b**.

K	Q	1a	1a_des	1b
	-2	-7.62E-01	2.21E+00	-1.35E+00
	-1	6.54E-01	3.80E+00	-3.77E+00
2	0	-8.53E-01	-3.13E+00	-3.41E+00
	1	2.02E-01	6.76E+00	-5.47E-01
	2	1.49E+00	-7.04E-02	8.76E-01
	-4	-4.60E-03	2.88E-02	-1.09E-02
	-3	-2.44E-02	1.54E-01	-4.73E-02
	-2	-2.81E-03	2.91E-02	4.32E-03
	-1	1.75E-03	-4.53E-02	4.96E-02
4	0	-1.92E-03	-9.63E-03	-3.76E-03
	1	5.47E-03	-7.32E-02	7.73E-03
	2	-2.43E-04	-2.31E-02	1.98E-03
	3	-4.48E-02	-2.43E-02	-1.99E-02
	4	3.48E-03	-2.21E-02	-1.30E-02
	-6	-2.33E-05	-1.37E-04	-6.53E-05
	-5	-8.58E-05	-4.08E-04	-1.11E-03
	-4	-2.74E-04	7.21E-05	-1.07E-04
	-3	-3.12E-04	-2.84E-06	2.52E-04
	-2	-2.55E-05	-3.40E-04	1.17E-04
	-1	-8.55E-05	1.15E-04	-2.64E-04
6	0	-2.19E-05	3.18E-05	2.24E-06
	1	-5.12E-06	1.55E-05	-3.24E-05
	2	-3.81E-05	9.72E-05	-1.41E-04
	3	-1.75E-04	-1.99E-05	-5.51E-05
	4	1.20E-05	-3.28E-05	-5.96E-05
	5	2.50E-04	1.90E-04	1.74E-04
	6	8.75E-05	-1.24E-04	3.05E-04

3.10 **Table S16**. The CASSCF/RASSI-SO/SINGLE_ANISO computed energy (cm^{-1}) of low lying states generated from $^7F_6$ for **2a, 2a-des** and **2b.**

2a	2a-des	2b
0.0	0.0	0.0
0.7	0.1	0.1
75.1	137.9	138.4
83.1	139.6	138.9
116.2	214.2	198.5
136.8	224.4	203.4
148.7	268.1	274.8
184.4	290.1	282.6
186.5	323.1	343.8
259.9	325.6	364.0
260.3	347.0	393.1
357.0	599.6	441.0
357.1	600.2	446.7

3.11 **Table S17.** The CASSCF/RASSI-SO/SINGLE_ANISO computed g_{zz} and m_J composition of first two pKDs (pseudo KDs) from $^7F_6$ for **2a, 2a-des** and **2b**.

2a		2a-des		2b	
g_{zz}	m_J composition	g_{zz}	m_J composition	g_{zz}	m_J composition
17.389	0.93|±6>	17.716	0.97|±6>	17.889	0.99|±6>
14.551	0.36|±5>+0.31|±3>+0.22|±1>	15.216	0.59|±5>+0.16|±3>+0.15|±4>	15.139	0.86|±5>

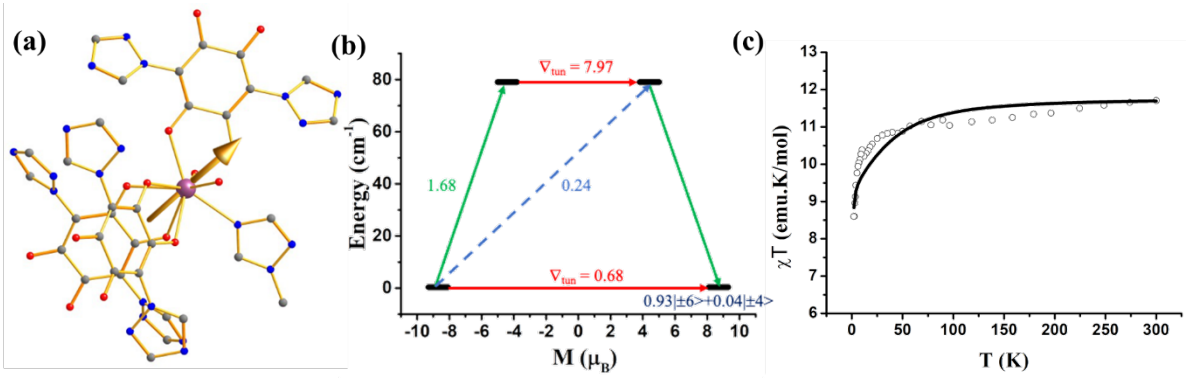

Figure S9. (a) The anisotropy axis of KD1 of **2a**. Colour code: Tb:maroon, O:red, N:blue, C:grey. Hydrogens are omitted for clarity. (b) The mechanism of magnetization relaxation of **2a**. The red arrow represents tunnel splitting via ground state and first excited state. The sky blue dotted arow represent the Orbach process. The green arrow shows possible mechanism of

magnetization relaxation. (c) A comparison of experimental and computed temperature dependent magnetization of **2a**. We have added TIP (temperature independent paramagnetism) value of 0.005 emu/mol to correct the experimental χT value of **2a**. A dipolar coupling (zJ) of -0.01 cm^{-1} was considered in our calculations to simulate the experimental magnetic data.

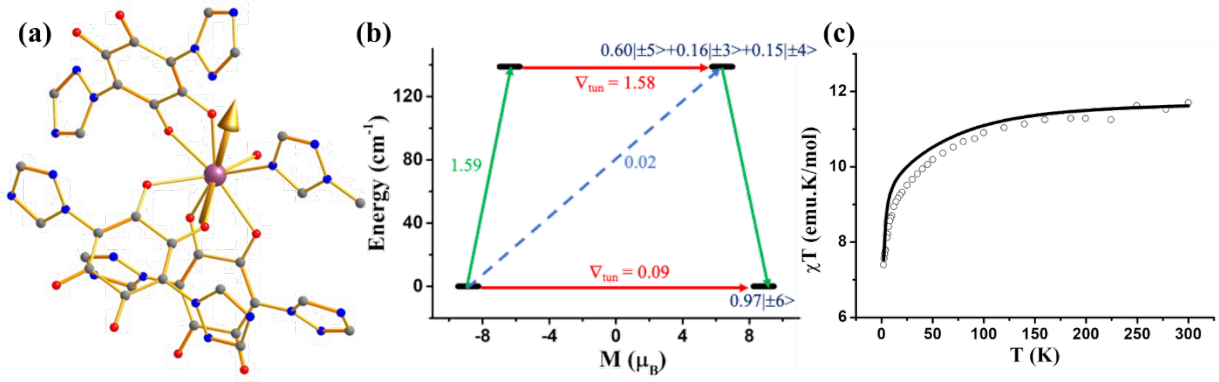

3.12 **Figure S10**. (a) The anisotropy axis of KD1 of **2a_des**. Colour code: Tb:maroon, O:red, N:blue, C:grey. Hydrogens are omitted for clarity. (b) The mechanism of magnetization relaxation of **2a_des**. The red arrow represents tunnel splitting via ground state and first excited state. The sky blue dotted arow represent the Orbach process. The green arrow shows possible mechanism of magnetization relaxation. (c) A comparison of experimental and computed temperature dependent magnetization of **2a_des**. We have added TIP (temperature independent paramagnetism) value of 0.005 emu/mol to correct the experimental χT value of **2a**. A dipolar coupling (zJ) of -0.05 cm^{-1} was considered in our calculations to simulate the experimental magnetic data.

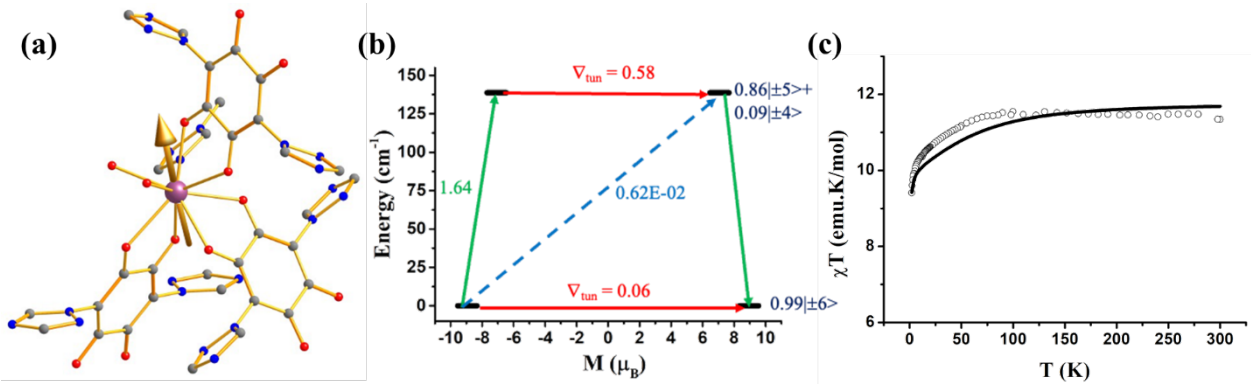

3.13 **Figure S11**. (a) The anisotropy axis of KD1 of **2b**. Colour code: Tb:maroon, O:red, N:blue, C:grey. Hydrogens are omitted for clarity. (b) The mechanism of magnetization relaxation of **2b**. The red arrow represents tunnel splitting via ground state and first excited state. The sky blue dotted arow represent the Orbach process. The green arrow shows possible mechanism of magnetization relaxation. (c) A comparison of experimental and computed temperature dependent magnetization of **2b**. We have added a scaling factor of 0.9 to correct the experimental χT value of **2b**. A dipolar coupling (zJ) of -0.01 cm^{-1} was considered in our calculations to simulate the experimental magnetic data.

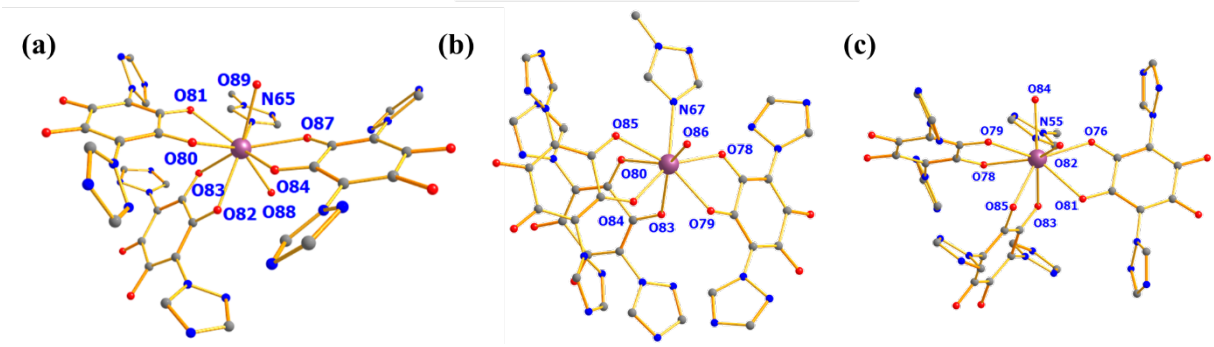

3.14 **Figure S12**. Loprop charge model of (a) **2a** (b) **2a_des** (c) **2b** for Table S19. Colour code: Tb:maroon, O:red, N:blue, C:grey. Hydrogens are omitted for clarity.

3.15 **Table S18**. The CASSCF computed Loprop charges metal and atoms in the first coordination sphere of **2a, 2a_des** and **2b**.

Atom	**2a**	**Atom**	**2a_des**	**Atom**	**2b**
Tb	2.5191	Tb	2.5167	Tb	2.5172
O80	-0.6908	O78	-0.7548	O76	-0.7557
O81	-0.7353	O79	-0.7058	O78	-0.7304
O82	-0.6657	O80	-0.7363	O79	-0.7093
O83	-0.7471	O83	-0.6778	O81	-0.6503
O84	-0.7064	O84	-0.7542	O82	-0.6934
O87	-0.6915	O85	-0.6974	O83	-0.7147
O88	-0.6910	O86	-0.6891	O84	-0.6968
O89	-06824	N67	-0.4360	O85	-0.6925
N65	-0.4287			N55	-0.3988

3.16 **Table S19**. The computed crystal field parameters (B_k^q; Stevens notation) in cm^{-1} obtained for **2a**, **2a_des** and **2b**.

k	**q**	**2a**	**2a_des**	**2b**
2	-2	3.01E+00	-1.71E+00	-1.50E+00

	-1	-7.23E-01	1.45E-01	2.31E+00
	0	-1.88E+00	-5.99E+00	-2.85E+00
	1	1.12E+00	-2.22E-01	-1.25E+00
	2	1.90E+00	-3.08E+00	1.44E+00
	-4	1.51E-03	-2.12E-02	-1.75E-02
	-3	4.81E-02	1.55E-02	3.97E-02
	-2	5.79E-03	4.22E-02	4.74E-03
	-1	1.66E-02	2.82E-03	-3.55E-02
4	0	-4.47E-03	3.78E-03	-5.80E-03
	1	-5.76E-03	9.70E-03	1.41E-02
	2	5.23E-03	2.14E-04	-1.25E-02
	3	5.27E-02	-1.60E-01	-1.61E-02
	4	-3.62E-02	-7.39E-02	9.97E-03
	-6	-1.24E-04	9.37E-05	3.85E-04
	-5	-2.25E-04	-3.67E-04	-2.42E-04
	-4	5.43E-05	-3.80E-05	-5.99E-05
	-3	1.33E-04	1.24E-04	-4.81E-05
	-2	2.23E-05	-2.12E-04	-2.94E-05
	-1	9.02E-06	-4.06E-05	3.22E-04
6	0	-3.35E-05	-1.93E-05	1.00E-05
	1	1.01E-05	1.53E-05	-7.35E-05
	2	-8.68E-05	3.21E-06	-8.29E-05
	3	2.45E-05	3.55E-04	2.04E-04
	4	-1.73E-04	2.47E-04	2.18E-05
	5	2.56E-04	5.85E-04	-1.11E-03
	6	5.23E-05	-2.85E-04	3.72E-05

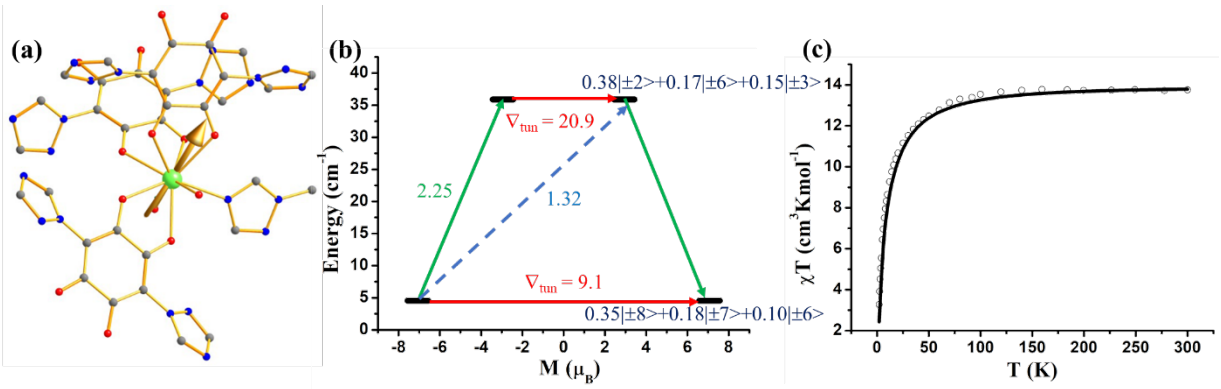

3.17 **Figure S13**. (a) The anisotropy axis of KD1 of **3a**. Colour code: Ho:green, O:red, N:blue, C:grey. Hydrogens are omitted for clarity. (b) The mechanism of magnetization relaxation of **3a**. The red arrow represents tunnel splitting via ground state and first excited state. The sky blue dotted arow represent the Orbach process. The green arrow shows possible mechanism of magnetization relaxation. (c) A comparison of experimental and computed temperature dependent magnetization of **3a**. The experimental data has been scaled by a factor of 0.90. A dipolar coupling (zJ) of -0.5 cm^{-1} was considered in our calculations to simulate the experimental magnetic data.

3.18 **Table S20**. The CASSCF/RASSI-SO/SINGLE_ANISO computed energy (cm^{-1}) of low lying states generated from $^5I_8$ for **3a, 3a-des** and **3b**.

3a	3a-des	3b
0.0	0.0	0.0
9.1	0.7	3.7
25.4	73.9	32.4
46.3	84.7	57.3
56.5	94.7	87.8
64.7	111.8	105.6
65.8	141.2	116.9
82.7	160.3	123.3
96.5	166.0	134.5
149.1	177.6	169.5
163.7	194.5	190.4
177.5	210.0	199.0
193.9	223.0	208.9
223.9	248.6	248.8
230.9	258.0	275.5
255.9	281.0	283.8
258.7	286.3	297.0

3.19 **Table S21**. The CASSCF/RASSI-SO/SINGLE_ANISO computed gzz and mJ composition of first two pKDs (pseudo KDs) from $^5I_8$ for **3a, 3a-des** and **3b**.

3a		**3a-des**		**3b**	
g_{zz}	m_J composition	g_{zz}	m_J composition	g_{zz}	m_J composition
14.140	0.35|±8>+0.18|±7>	18.807	0.84|±8>+0.03|±6>	16.967	0.62|±8>+0.16|±5>
9.583	0.38|±2>+0.17|±6>	14.393	0.34|±3>+0.19|±7>	13.489	0.40|±4>+0.17|±5>

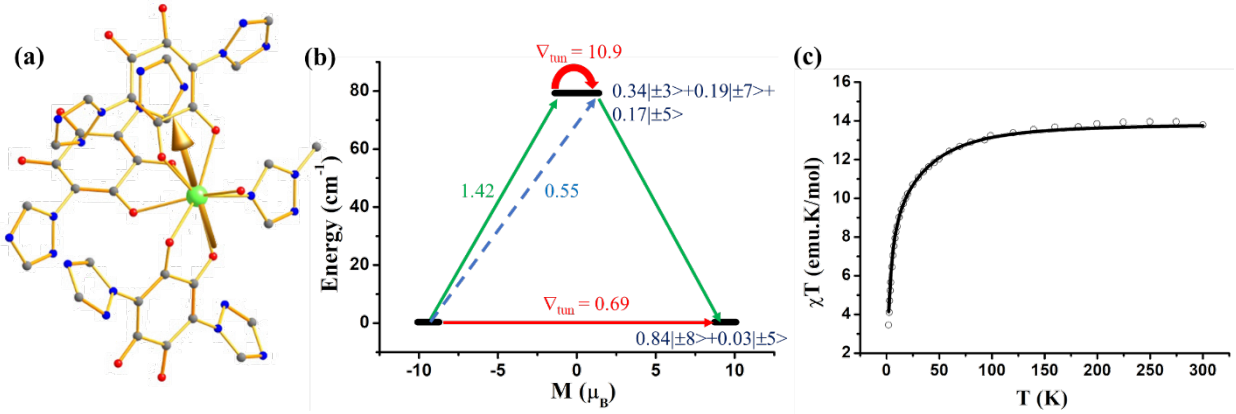

3.20 **Figure S14**. (a) The anisotropy axis of KD1 of **3a_des**. Colour code: Ho:green, O:red, N:blue, C:grey. Hydrogens are omitted for clarity. (b) The mechanism of magnetization relaxation of **3a_des**. The red arrow represents tunnel splitting via ground state and first excited state. The sky blue dotted arow represent the Orbach process. The green arrow shows possible mechanism of magnetization relaxation. (c) A comparison of experimental and computed temperature dependent magnetization of **3a_des**. The experimental data has been scaled by a factor of 0.80. A dipolar coupling (zJ) of -0.7 cm^{-1} was considered in our calculations to simulate the experimental magnetic data.

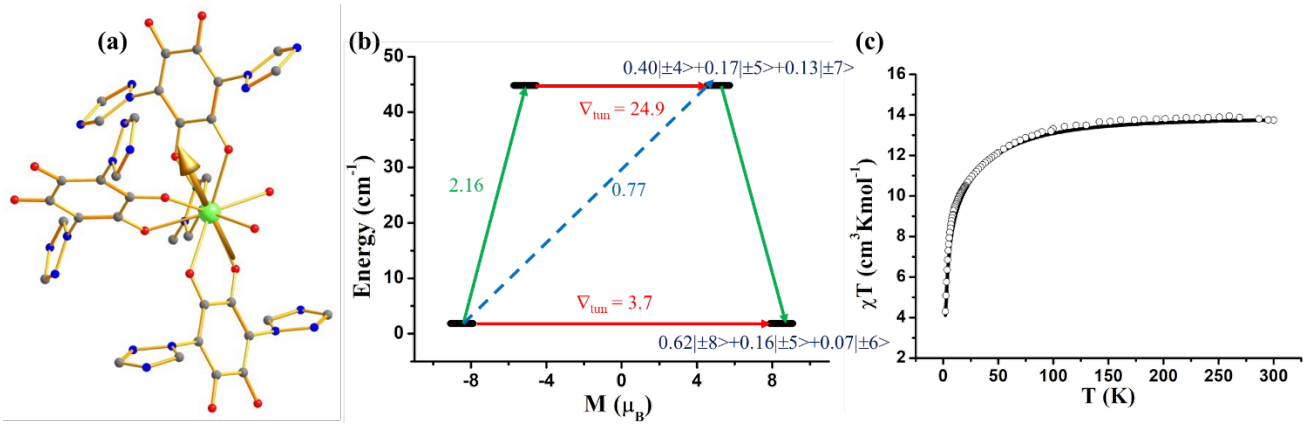

3.21 **Figure S15**. (a) The anisotropy axis of KD1 of **3b.** Colour code: Ho:green, O:red, N:blue, C:grey. Hydrogens are omitted for clarity. (b) The mechanism of magnetization relaxation of **3b**. The red arrow represents tunnel splitting via ground state and first excited state. The sky blue dotted arow represent the Orbach process. The green arrow shows possible mechanism of magnetization relaxation. (c) A comparison of experimental and computed temperature dependent magnetization of **3b**. A dipolar coupling (zJ) of -0.4 cm^{-1} was considered in our calculations to simulate the experimental magnetic data.

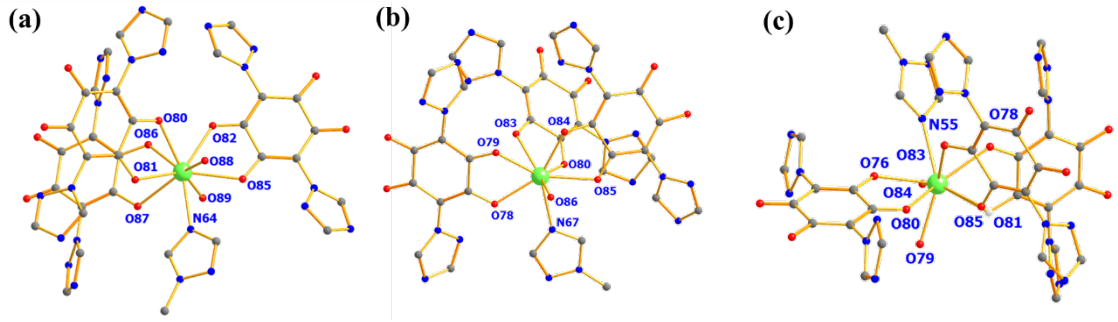

3.22 **Figure S16**. Loprop charge model of (a) 3a (b) 3a_des (c) 3b for Table S24. Colour code: Ho:green, O:red, N:blue, C:grey. Hydrogens are omitted for clarity.

3.23 **Table S22**. The CASSCF computed Loprop charges metal and atoms in the first coordination sphere of **3a, 3a_des and 3b.**

Atom	**3a**	**Atom**	**3a_des**	**Atom**	**3b**
Ho	2.5145	Ho	2.5150	Ho	2.5128
O80	-0.6650	O78	-0.7485	O76	-0.7463
O81	-0.7328	O79	-0.7178	O78	-0.7193
O82	-0.6882	O80	-0.7338	O79	-0.7143
O85	-0.7238	O83	-0.6791	O80	-0.6515
O86	-0.6802	O84	-0.7534	O81	-0.7224
O87	-0.7338	O85	-0.6923	O83	-0.6936
O88	-0.7023	O86	-0.6974	O84	-0.6961
O89	-0.6877	N67	-0.4346	O85	-0.7144
N64	-0.4424			N55	-0.3983

3.24 **Table S23**. The computed crystal field parameters (B_k^q; Stevens notation) in cm^{-1} obtained for **3a, 3a_des** and **3b**.

k	**q**	**3a**	**3a_des**	**3b**
2	-2	-1.05E-01	4.87E-02	1.74E-01
	-1	4.96E-01	-9.31E-01	-1.75E-01
	0	-3.13E-01	-5.84E-01	-5.45E-01
	1	-4.24E-04	2.76E-01	2.26E-01

	2	-3.92E-01	-5.61E-01	-2.99E-01
4	-4	4.52E-05	-6.20E-03	3.82E-03
	-3	4.42E-03	-6.49E-03	4.23E-03
	-2	-9.92E-04	-5.08E-03	-1.39E-03
	-1	3.13E-03	5.46E-03	8.95E-03
	0	-7.45E-04	-2.23E-03	1.07E-04
	1	-9.54E-04	3.15E-03	-7.38E-03
	2	-1.57E-03	-9.56E-03	-1.98E-03
	3	1.74E-02	1.34E-02	5.03E-03
	4	4.78E-03	-5.14E-03	-8.55E-04
6	-6	-1.19E-04	-9.38E-05	-1.39E-04
	-5	-1.86E-04	-1.38E-04	-1.05E-03
	-4	-6.14E-05	7.58E-05	-1.29E-04
	-3	2.33E-04	2.57E-04	4.68E-05
	-2	-1.78E-05	9.74E-05	-1.46E-04
	-1	-7.70E-05	1.78E-05	2.52E-06
	0	9.89E-06	-1.14E-05	-2.07E-05
	1	1.94E-04	9.21E-05	-4.00E-05
	2	1.40E-04	2.35E-05	4.36E-05
	3	-3.66E-05	-2.72E-04	4.07E-04
	4	-2.70E-04	-8.18E-05	-5.87E-06
	5	-7.70E-04	-3.98E-05	-4.30E-04
	6	-2.92E-05	-2.86E-05	-1.45E-04

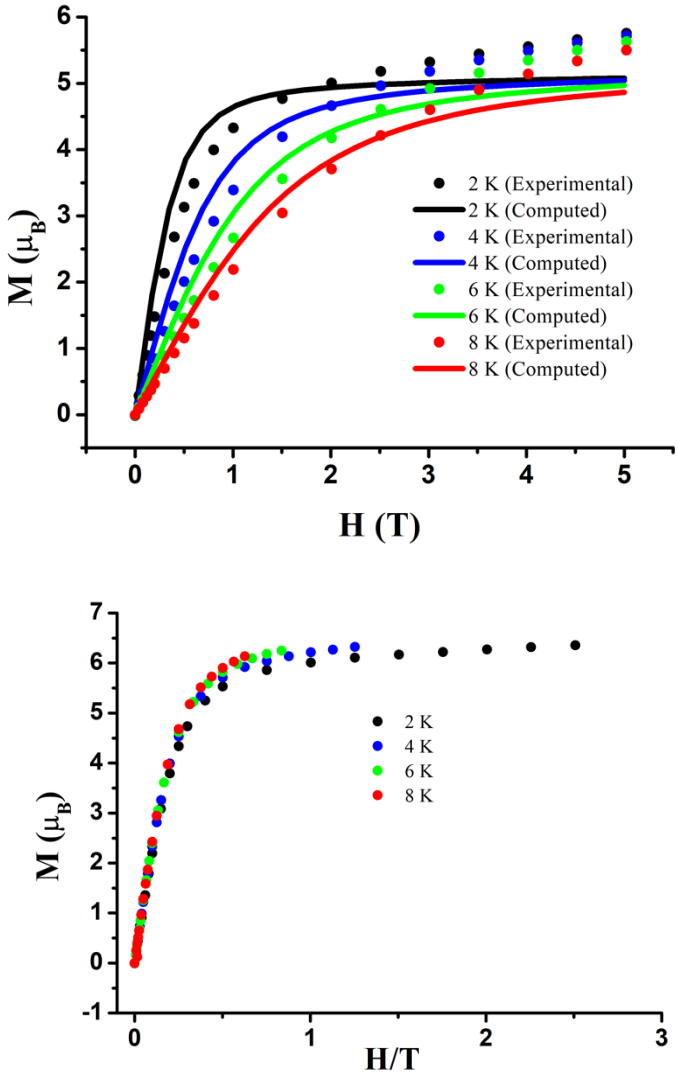

3.25 **Figure S17**. Magnetization (M) versus field (H) of **1a** from 2 to 8 K.

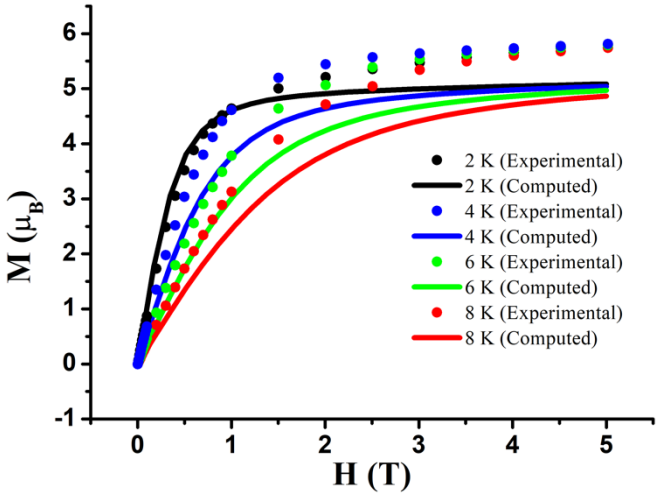

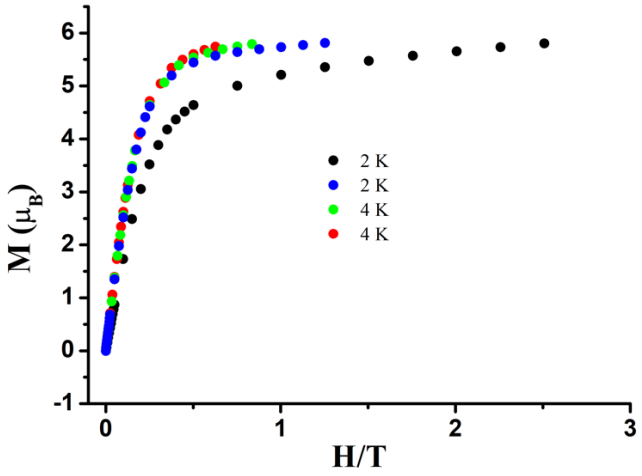

3.26 **Figure S18**. Magnetization (M) versus field (H) of **1a_des** from 2 to 8 K.

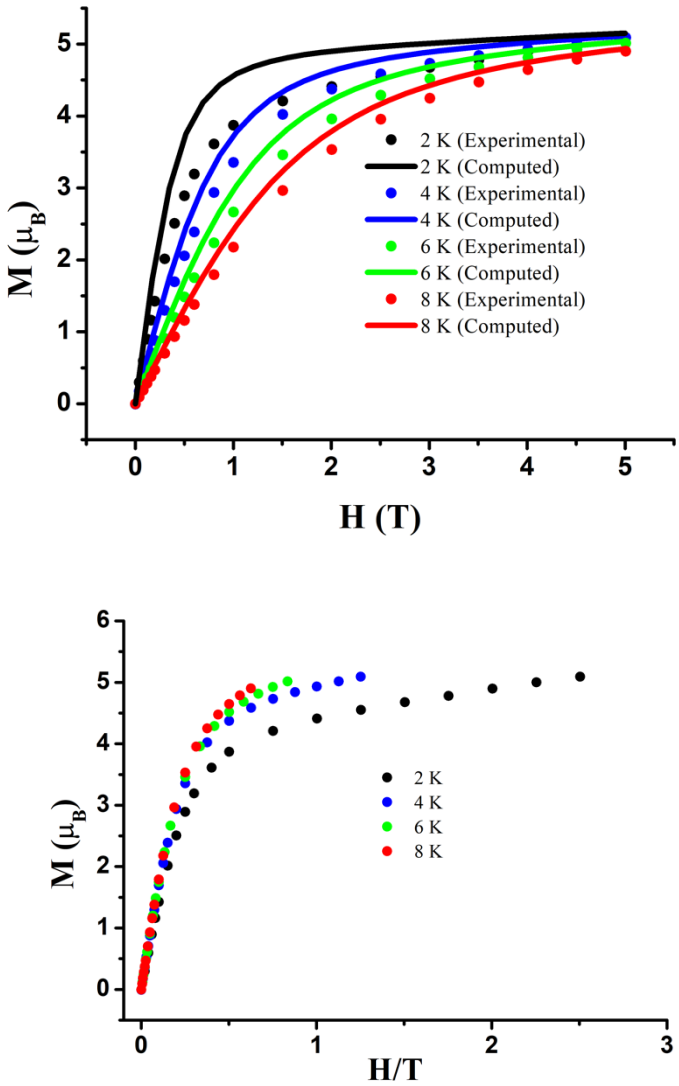

3.27 **Figure S19**. Magnetization (M) versus field (H) of **1b** from 2 to 8 K.

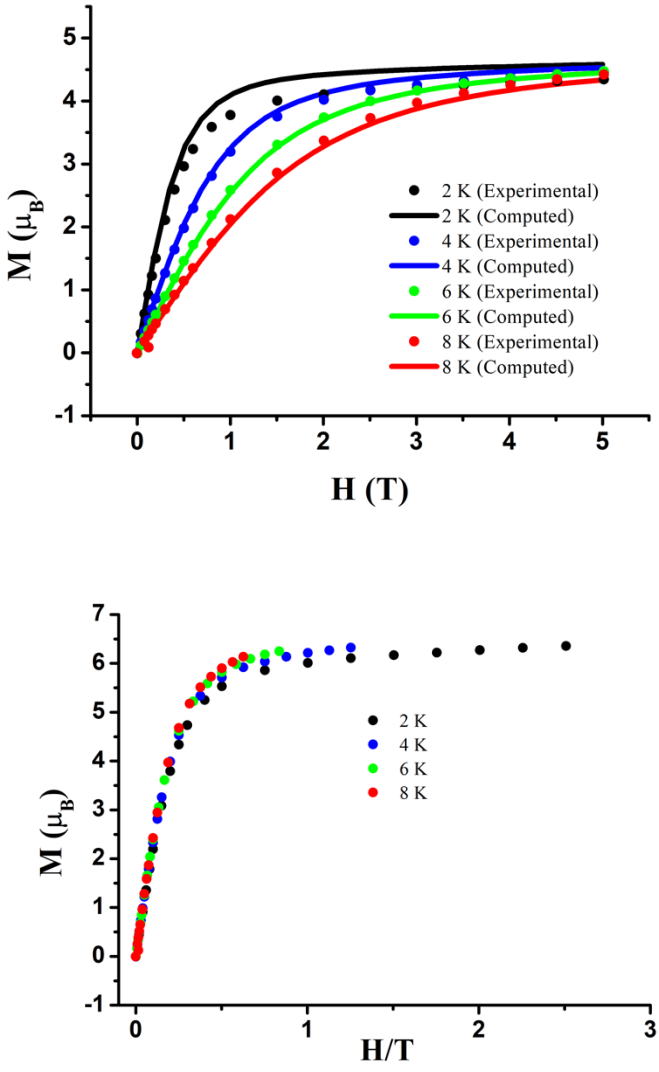

3.28 **Figure S20**. Magnetization (M) versus field (H) of **2a** from 2 to 8 K.

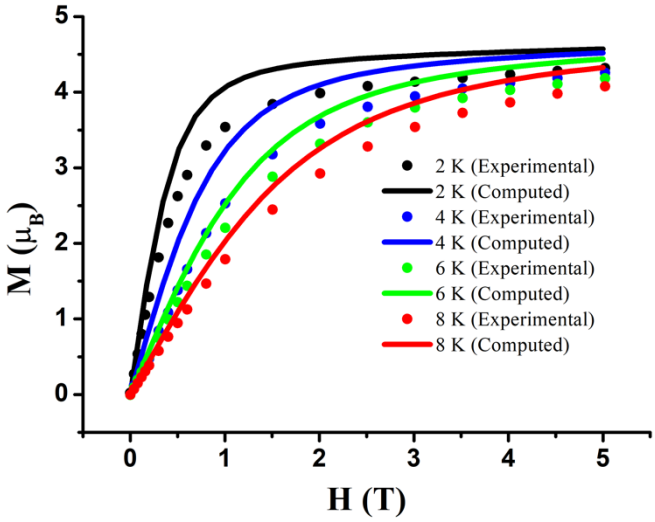

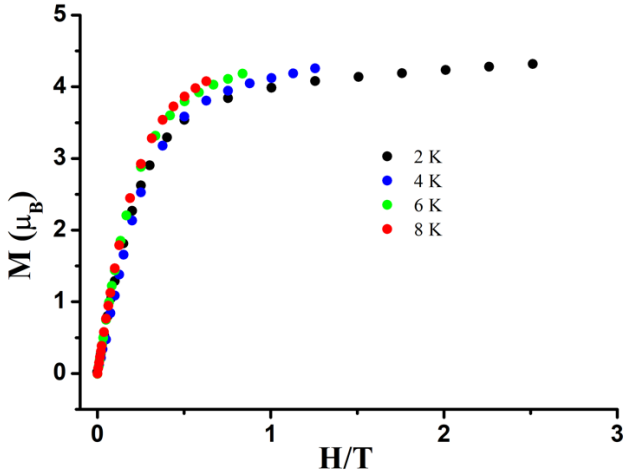

3.29 **Figure S21**. Magnetization (M) versus field (H) of **2a_des** from 2 to 8 K.

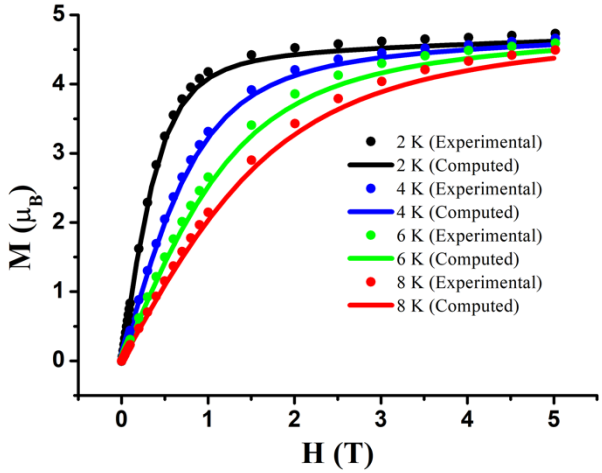

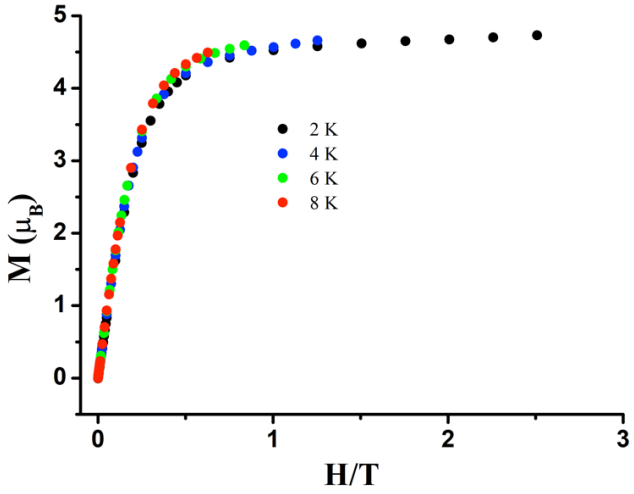

3.30 **Figure S22**. Magnetization (M) versus field (H) of **2b** from 2 to 8 K.

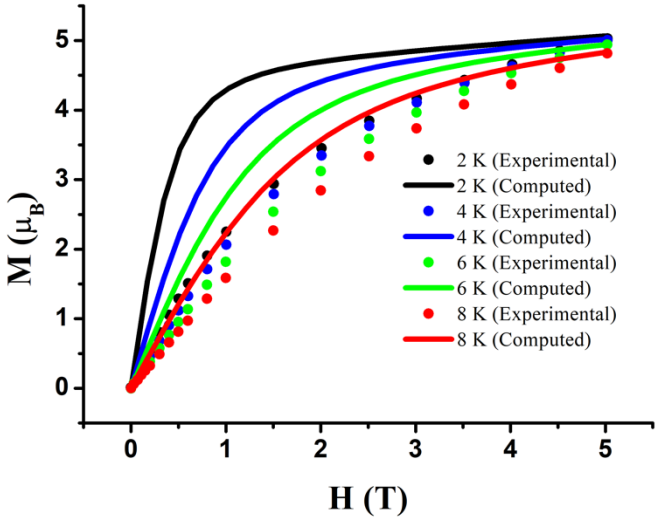

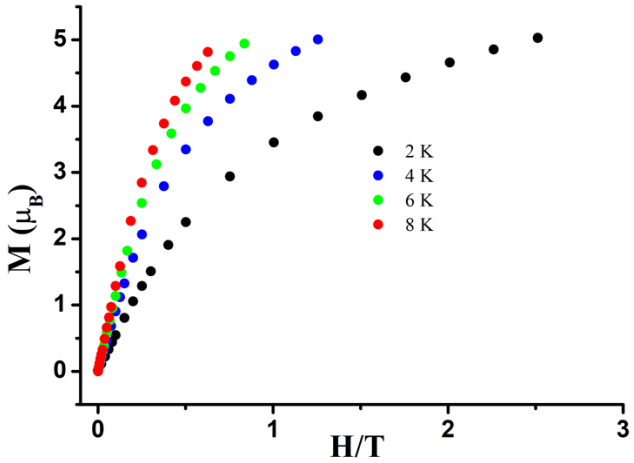

3.31 **Figure S23**. Magnetization (M) versus field (H) of **3a** from 2 to 8 K.

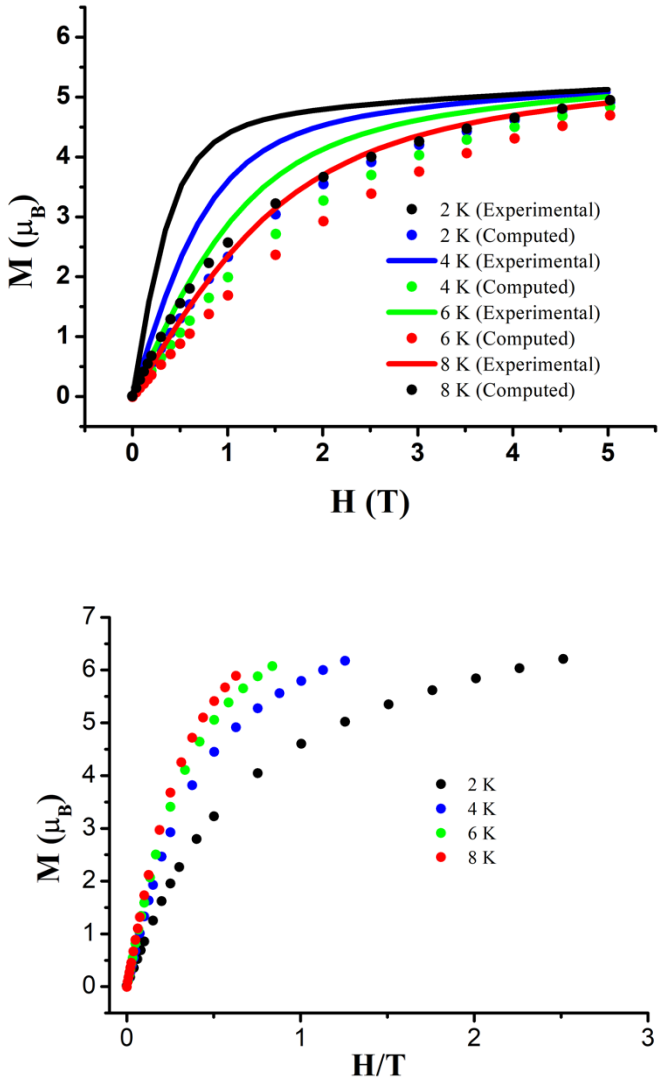

3.32 **Figure S24**. Magnetization (M) versus field (H) of **3a_des** from 2 to 8 K.

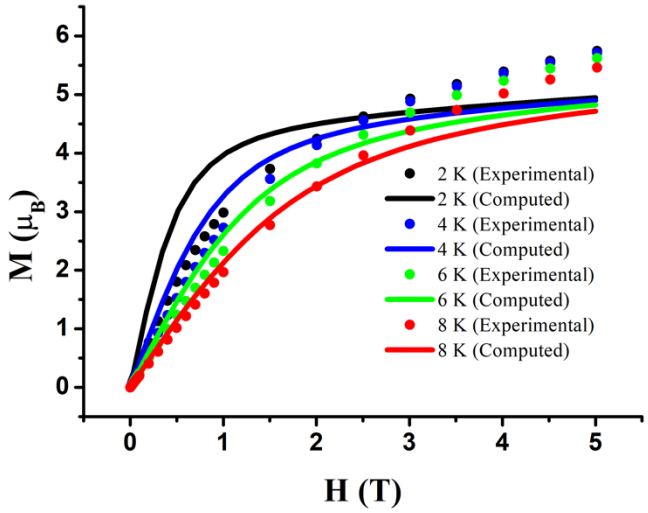

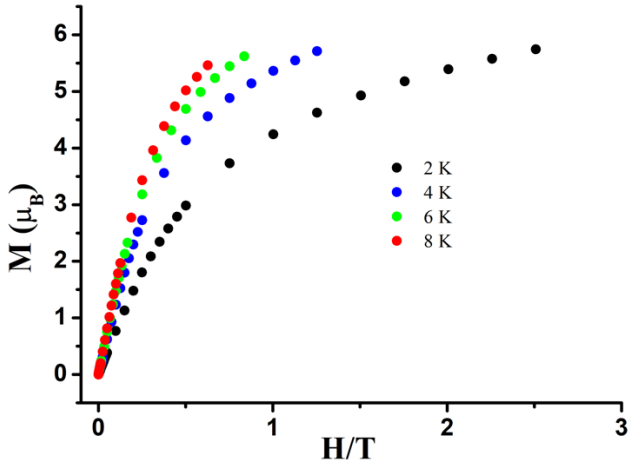

3.33 **Figure S25**. Magnetization (M) versus field (H) of **3b** from 2 to 8 K.

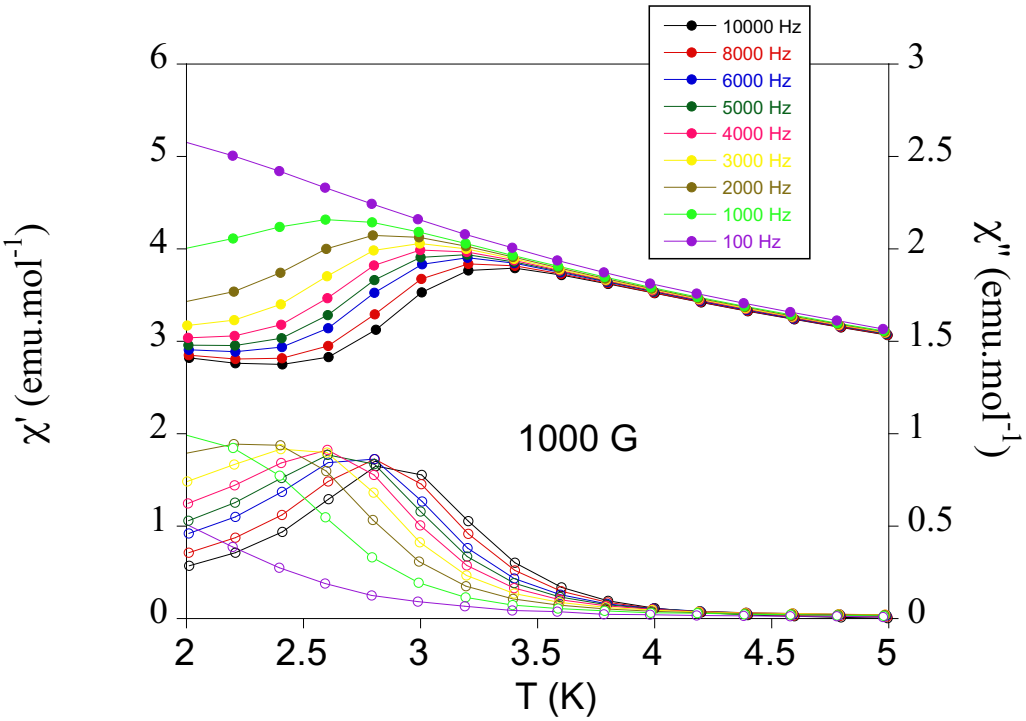

3.34 **Figure S26**. Temperature dependence of χ' (full symbols) and χ'' (empty symbols) of **1a** measured in contact with the mother liquor in an applied dc field of 0.1 T at frequencies in the range 100 to 10000 Hz.

a)

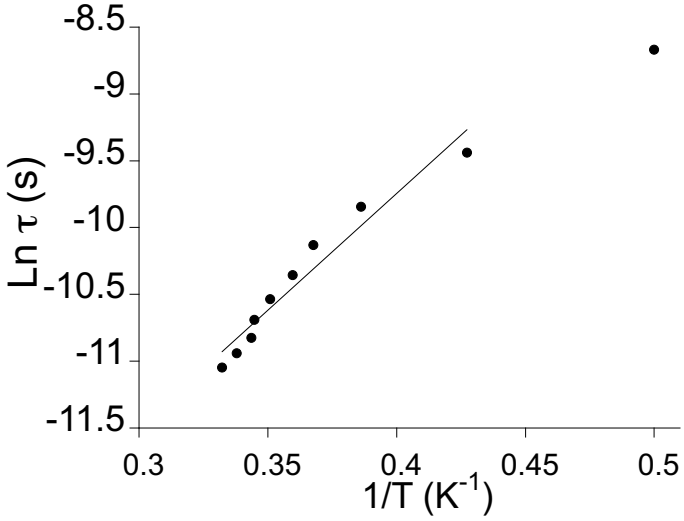

b)

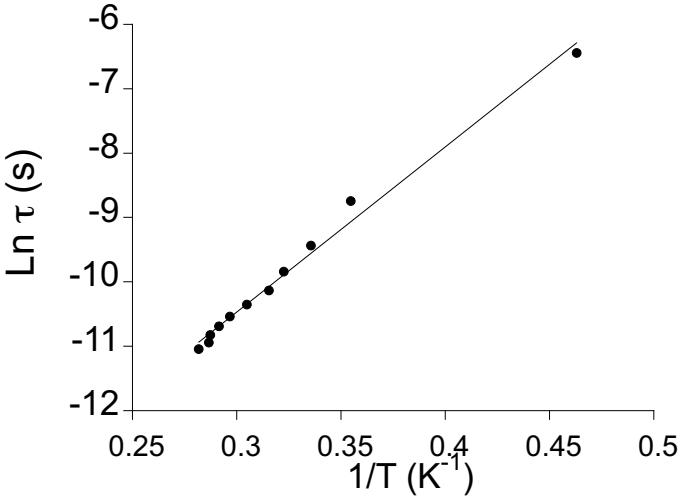

c)

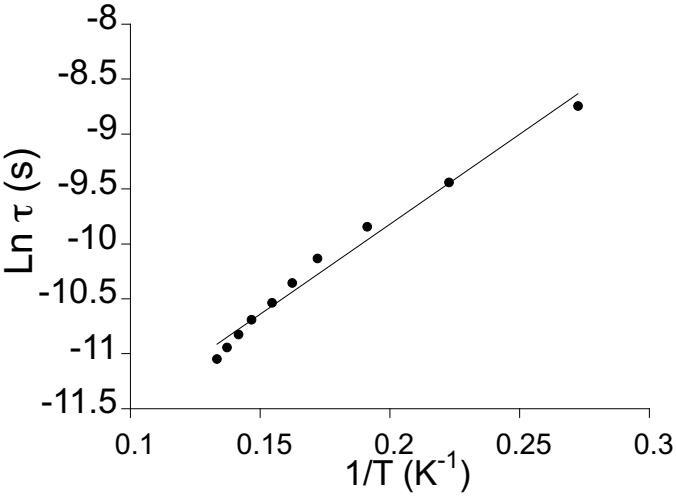

3.35 **Figure S27**. Plot of Ln τ versus T-1 for **1a_des** (a), **1b** (b) and **2b** (c).

a)

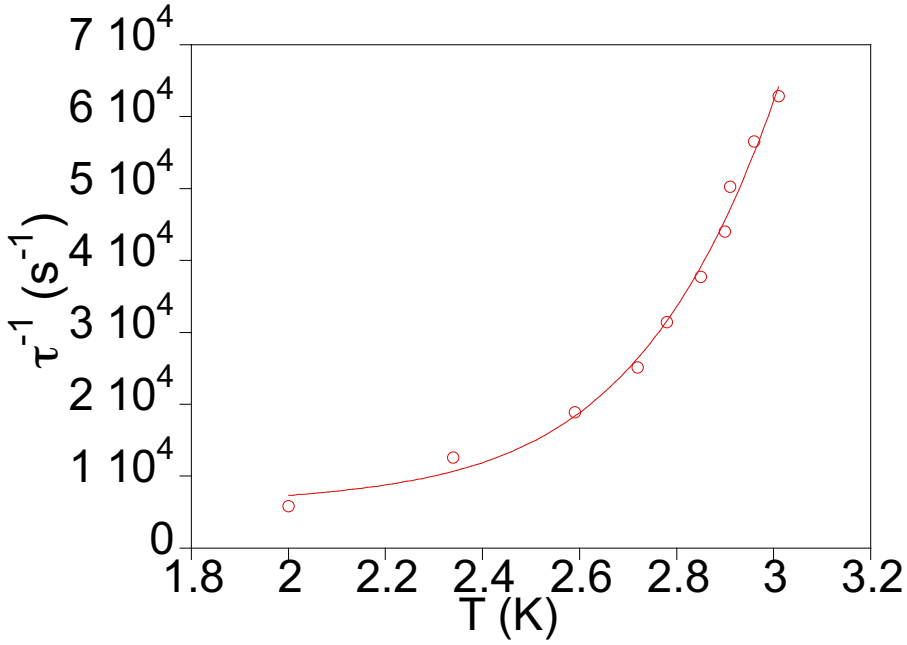

b)

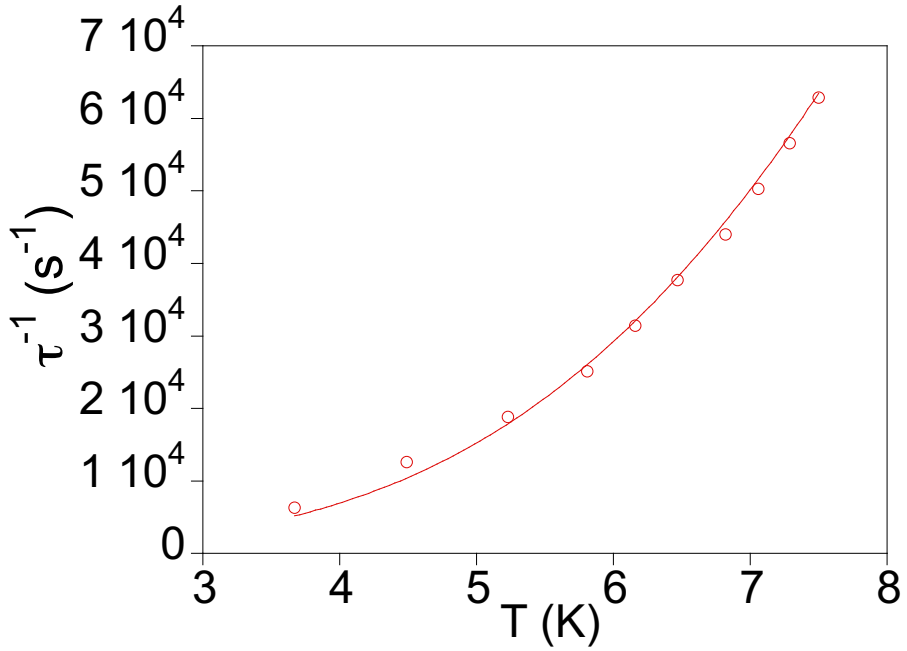

3.36 **Figure S28**. Thermal dependence of the relaxation time of **1a_des** (a) and **2b** (b) and best fit from two terms mechanism described in text.

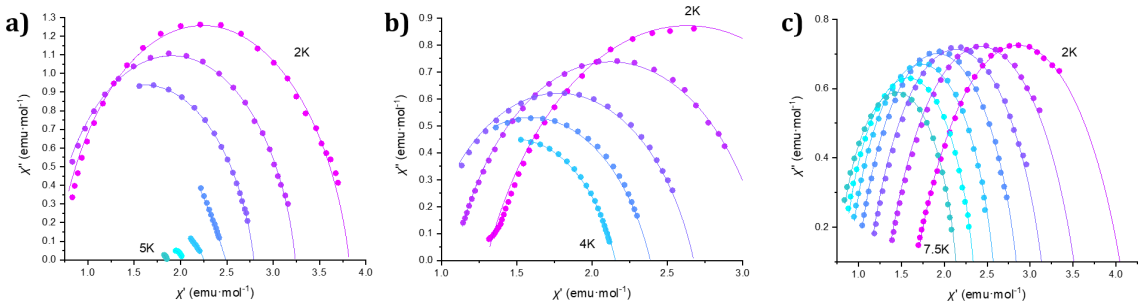

3.37 **Figure S29**. Cole-Cole plots of **1a_des** (a) and **1b** (b) and **2b** (c) measured at the same temperatures as **Figures 10-12** under an applied dc field of 0.1 T. Solid lines represent the best fitting of the experimental data to a Cole-Cole function.

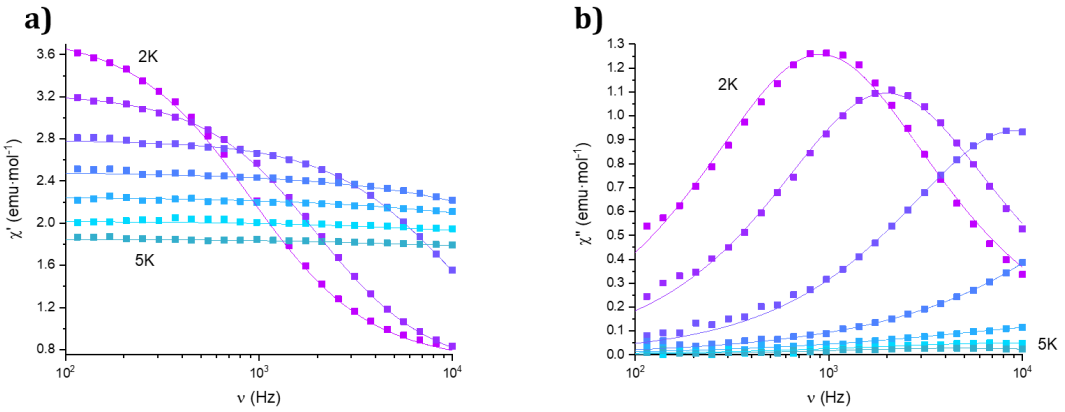

3.38 **Figure S30**. AC susceptibility in an applied dc field of 0.1 T of **1a_des** measured as a function of the frequency at the different temperatures (2.0, 2.5, 3.0, 3.5, 4.0, 4.5 and 5.0 K). (a): Real component. (b): Imaginary component. Solid lines represent the best fitting of the experimental data to a Cole-Cole function.

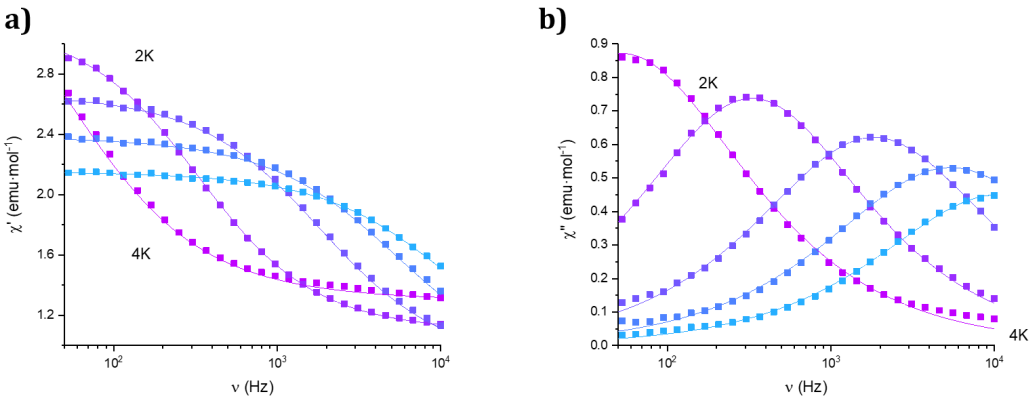

3.39 **Figure S31**. AC susceptibility in an applied dc field of 0.1 T of **1b** measured as a function of the frequency at the different temperatures (2.0, 2.5, 3.0, 3.5 and 4.0 K). (a): Real component. (b): Imaginary component. Solid lines represent the best fitting of the experimental data to a Cole-Cole function.

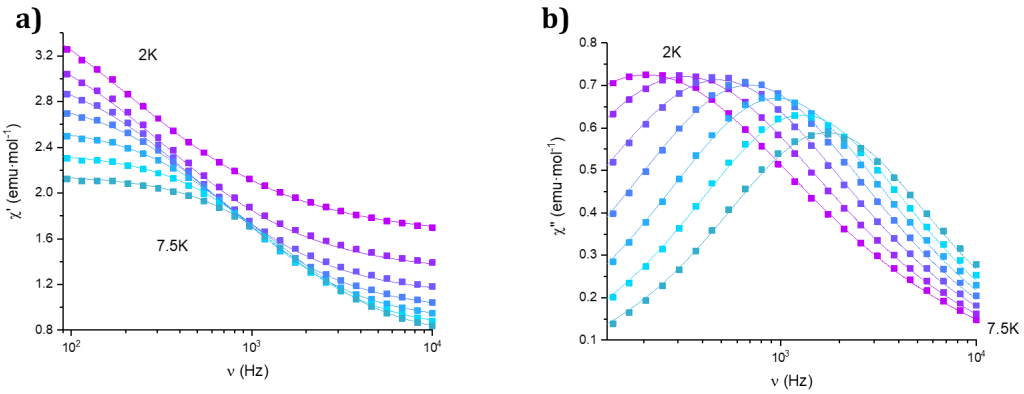

3.40 **Figure S32**. AC susceptibility in an applied dc field of 0.1 T **2b** measured as a function of the frequency at the different temperatures (2.0, 2.5, 3.0, 3.5, 4.0, 4.5, 5.0, 5.5, 6.0, 6.5, 7.0 and 7.5 K). (a): Real component. (b): Imaginary component. Solid lines represent the best fitting of the experimental data to a Cole-Cole function.